

Potentiometric and UV–Visible Spectroscopic Studies of Cobalt(II), Copper(II), and Nickel(II) Complexes with *N,N'*-(*S,S*)-Bis[1-carboxy-2-(imidazol-4-yl)ethyl]ethylenediamine

João G. Martins,[†] Paula Gameiro,[‡] M. Teresa Barros,[§] and Helena M. V. M. Soares^{*,†}

REQUIMTE - Departamento de Engenharia Química, Faculdade de Engenharia, Universidade do Porto, 4200-465, Porto, Portugal, REQUIMTE - Departamento de Química, Faculdade de Ciências, Universidade do Porto, 4169-007, Porto, Portugal, and REQUIMTE, Departamento de Química, Faculdade de Ciências e Tecnologia, Universidade Nova de Lisboa, 2829-516 Caparica, Portugal

Solution equilibrium studies on the M(II) [Co(II), Cu(II), and Ni(II)] *N,N'*-(*S,S*)-bis[1-carboxy-2-(imidazol-4-yl)ethyl]ethylenediamine (BCIEE) systems have been performed by pH potentiometry and UV–visible spectroscopy in 0.1 M KCl at 25 °C. Overall stability constants were established, by potentiometry, for all M(II)–BCIEE systems. Results evidenced the formation of a highly stable ML complex with all M(II)–BCIEE systems, which is the dominant species over a wide range of pH, plus different protonated, MH₂L, complexes. From potentiometric and spectroscopic results, it was shown that, for ML complexes, BCIEE binds to Co(II) or Cu(II) through the two amine and two imidazole groups in the chelate plane and through the carboxyl groups in the apical positions, while the coordination of the NiL complex is assumed to be by four nitrogen groups in the plane. In the case of MHL complexes in the Cu(II)–BCIEE and Ni(II)–BCIEE systems, BCIEE behaves as a tridentate ligand [via COO[−], NH₂, and N(Im) groups] coordinating to the metal ion in the chelate plane. Results also suggest that BCIEE behaves as a bidentate ligand [via COO[−] and N(Im) or via NH₂ and N(Im) groups], forming an equilibrium mixture of two CuH₂L structures for the Cu(II)–BCIEE system.

1. Introduction

Aminopolycarboxylates (APCAs) and organophosphonates are well-known effective chelators and the most commonly used as complexing agents. Because of their excellent binding capacity, they have been widely used as chelating agents in many industrial processes and products for years.

APCAs, such as ethylenediaminetetraacetic acid (EDTA) and diethylenetriaminepentaacetic acid (DTPA), are used in huge quantities worldwide. The available data on production, sales, and application of complexing agents are incomplete.¹ The global consumption of these APCAs (EDTA and DTPA) is roughly about 200 000 tons per year and is increasing.² However, all of these traditional chelating agents are essentially nonbiodegradable. Therefore, their accumulation in the environment is becoming a matter of great concern. EDTA, for example, occurs at higher concentrations in European surface waters than any other identified anthropogenic organic compound.³ Chelating agents have the potential to perturb the natural speciation of metals and to influence metal bioavailability. Their presence at high concentrations may lead to the remobilization of metals from sediments and aquifers, consequently posing a risk to groundwater and drinking water.³ Thus, there is a pressing requirement to replace EDTA and similar ligands with readily biodegradable alternatives.

Recently, much effort has been put into finding new chelating agents that are more environmentally friendly and capable of

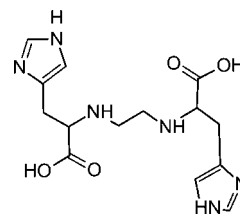


Figure 1. Structure of *N,N'*-(*S,S*)-bis[1-carboxy-2-(imidazol-4-yl)ethyl]ethylenediamine (BCIEE).

substituting the traditional ones. Synthesis,^{4,5} complexation,^{6–8} and biodegradation⁹ studies of potential biodegradable chelating agents have been reported in the literature. One of these candidates is the [*S,S*]-stereoisomer of ethylenediaminedisuccinic acid, *S,S*-EDDS, and its biodegradability in domestic sludge has been demonstrated.¹⁰

In recent years, our group has been involved in the development of environmentally friendly complexing agents.^{11,12} For realizing the environmental biodegradation criterion, which is dependent upon commonly occurring ubiquitous bacteria, we synthesized APCAs based on the enantiopure L-amino-acids (the isomeric form more abundant in living organisms,¹³ expecting that their degradation products will be more easily accepted into the host environment¹⁴) attached to an ethylenediamine central moiety originating secondary amines, which are potentially biodegradable¹⁵ and good candidates as chelating agents.

With this in mind, the *N,N'*-(*S,S*)-bis[1-carboxy-2-(imidazol-4-yl)ethyl]ethylenediamine (BCIEE) ligand (Figure 1), a 1,2-ethylene disubstituted derivative of L-histidine, should be a strong chelator since it has six possible coordinating atoms [four nitrogen (two

* Corresponding author. E-mail: hsoares@fe.up.pt; phone: +351 22 508 1650; fax: +351 22 508 1449.

[†] Faculdade de Engenharia, Universidade do Porto.

[‡] Faculdade de Ciências, Universidade do Porto.

[§] Universidade Nova de Lisboa.

saturated amines and two imidazolyl groups) plus two carboxylic acids], which can form several membered rings. In addition, nitrogen atoms from imidazolyl groups are more effective than saturated amines due to the lower protonation constants.¹⁶

Recently, the synthesis of this compound, as well as their protonation constants and Eu(III) formation constants were described in the literature.^{17,18} However, as far as we know, no data are available for other important metal ions in the literature. Since the compound BCIEE seems to have the required structural characteristics for being a potential green chelator agent and following our earlier studies on the coordination behavior of environmentally friendly complexing agents toward transition metal ions,^{11,12} we decided to study its complexing properties with several metal ions.

Under this context, BCIEE was synthesized on the basis of the method described by Miyake et al.¹⁷ Then, the formation constants of the complexes in aqueous solution with BCIEE and the Co(II), Cu(II), and Ni(II) metal ions were determined by potentiometry. Spectroscopic properties of the Co(II), Cu(II), and Ni(II) complexes were characterized by means of UV–visible (UV–vis) spectroscopy. Further work related to the biodegradability of BCIEE should be carried out.

2. Materials and Methods

2.1. Potentiometric Measurements. The potentiometric titrations were performed with a personal computer (PC) controlled system as previously described.¹¹

All measurements were performed on solutions adjusted to an ionic strength of 0.1 M with KCl in a Methrom (Herisau, Switzerland) jacketed glass vessel, equipped with a magnetic stirrer, and thermostated at $(25.0 \pm 0.1)^\circ\text{C}$ using a water bath. A stream of purified nitrogen was used as the inert atmosphere in the titration cells to degas all solutions before the titrations. Oxygen and carbon dioxide were excluded from the reaction mixture by maintaining a slight positive pressure of purified nitrogen in the titration cell.

The glass electrode calibration, in terms of hydrogen ion concentration, was accomplished by the addition of a standardized solution of potassium hydroxide to a standardized solution of hydrochloric acid (both solutions adjusted to the ionic strength of 0.1 M). From this potentiometric titration, the values of E° and response slope were obtained by fitting a straight line to the experimental points collected around pH 2 and 11.

The metal stability constants of BCIEE with metal ions Co(II), Cu(II), and Ni(II) were all determined by direct potentiometric titrations. For all systems, monotonic titrant volume additions of standardized KOH were made, and the potential was recorded as a function of the added volume. For all the $M(\text{BCIEE})_x(\text{OH})_y$ systems studied, pH–potentiometric titrations were performed using fixed total ligand-to-total-metal-ion concentration ($[\text{L}_\text{T}]:[\text{M}_\text{T}]$) ratios over a wide pH range. The $[\text{L}_\text{T}]:[\text{M}_\text{T}]$ ratios used to characterize $M(\text{BCIEE})_x(\text{OH})_y$ systems, as well as the pH range used in the potentiometric titrations, are compiled in Table 1.

The simulation and optimization procedures of potentiometric data were done using the ESTA program^{19,20} as previously described.¹¹ During the refinement operations of the different metal–BCIEE systems studied, the water and BCIEE protonation constants, as well as all known formation constants for metal hydroxide species, $M_x(\text{OH})_y$, were kept fixed (Table 2).

2.2. UV–vis Measurements. The UV–vis absorption spectra for the $M(\text{BCIEE})_x(\text{OH})_y$, $M = \text{Co(II)}$, Cu(II) , and Ni(II) , systems were recorded at 25.0°C on a Varian Cary 50 Bio UV–vis

Table 1. Experimental Conditions Used in the Determination of Global Stability Constants in $M\text{L}_x(\text{OH})_y$ Systems, By Glass Electrode Potentiometry (GEP) and UV–vis Measurements, at 25°C and $\mu = 0.1 \text{ mol}\cdot\text{L}^{-1}$ (KCl)

technique	metal	$[\text{L}_\text{T}]:[\text{M}_\text{T}]$	$[\text{M}_\text{T}]$	pH range
			$\text{mol}\cdot\text{L}^{-1}$	
GEP	Cu	1	$1.0\cdot 10^{-3}$	2.0 to 11.5
	Co	1	$1.0\cdot 10^{-3}$	
	Ni	1	$1.0\cdot 10^{-3}$	
UV–vis	Cu	1	$1.0\cdot 10^{-3}$	2.0 to 6.5
	Co	1	$1.0\cdot 10^{-2}$	1.5 to 7.0
	Ni	1	$1.0\cdot 10^{-2}$	2.0 to 7.9

Table 2. Protonation Constants for Water and BCIEE and Overall Stability Constants for $M(\text{II})$ Complexes with OH^- at 25.0°C

	equilibrium	$\log \beta$	μ ($\text{mol}\cdot\text{L}^{-1}$)	refs
water	$\text{H}^+ + \text{OH}^- \rightleftharpoons \text{H}_2\text{O}$	13.78	0.1	23
BCIEE	$\text{L}^{2-} + \text{H}^+ \rightleftharpoons \text{HL}^-$	9.24	0.1	18
	$\text{L}^{2-} + 2\text{H}^+ \rightleftharpoons \text{H}_2\text{L}$	16.48	0.1	18
	$\text{L}^{2-} + 3\text{H}^+ \rightleftharpoons \text{H}_3\text{L}^+$	22.52	0.1	18
	$\text{L}^{2-} + 4\text{H}^+ \rightleftharpoons \text{H}_4\text{L}^{2+}$	27.33	0.1	18
	$\text{L}^{2-} + 5\text{H}^+ \rightleftharpoons \text{H}_5\text{L}^{3+}$	30.07	0.1	18
cobalt	$\text{Co}^{2+} + \text{OH}^- \rightleftharpoons \text{Co}(\text{OH})^+$	4.3	0.0	23
	$\text{Co}^{2+} + 2\text{OH}^- \rightleftharpoons \text{Co}(\text{OH})_2$	9.2	0.0	23
	$\text{Co}^{2+} + 3\text{OH}^- \rightleftharpoons \text{Co}(\text{OH})_3^-$	10.5	0.0	23
	$\text{Co}(\text{OH})_2(\text{s}) \rightleftharpoons \text{Co}^{2+} + 2\text{OH}^-$	-14.9	0.0	23
	copper	$\text{Cu}^{2+} + \text{OH}^- \rightleftharpoons \text{Cu}(\text{OH})^+$	6.1	0.1
$\text{Cu}^{2+} + 2\text{OH}^- \rightleftharpoons \text{Cu}(\text{OH})_2$		11.8	0.0	36
$\text{Cu}^{2+} + 3\text{OH}^- \rightleftharpoons \text{Cu}(\text{OH})_3^-$		14.5	1.0	36
$\text{Cu}^{2+} + 4\text{OH}^- \rightleftharpoons \text{Cu}(\text{OH})_4^{2-}$		15.6	1.0	36
$\text{Cu}(\text{OH})_2(\text{s}) \rightleftharpoons \text{Cu}^{2+} + 2\text{OH}^-$		-18.9	1.0	23
nickel	$\text{Ni}^{2+} + \text{OH}^- \rightleftharpoons \text{Ni}(\text{OH})^+$	3.7	0.1	23
	$\text{Ni}^{2+} + 2\text{OH}^- \rightleftharpoons \text{Ni}(\text{OH})_2$	9.0	0.0	23
	$\text{Ni}^{2+} + 3\text{OH}^- \rightleftharpoons \text{Ni}(\text{OH})_3^-$	12.0	0.0	23
	$\text{Ni}(\text{OH})_2(\text{s}) \rightleftharpoons \text{Ni}^{2+} + 2\text{OH}^-$	-15.1	0.0	23

spectrophotometer, using standard 1 cm quartz cells. For all $M(\text{BCIEE})_x(\text{OH})_y$ systems, the spectra were scanned from (200 to 1100) nm.

The $[\text{L}_\text{T}]:[\text{M}_\text{T}]$ ratios used to characterize the $M(\text{BCIEE})_x(\text{OH})_y$ systems, as well as the pH range used in the UV–vis spectroscopic measurements, are compiled in Table 1. For this purpose, a stock solution of each $[\text{L}_\text{T}]:[\text{M}_\text{T}]$ system was prepared. The pH of the batch solutions was changed by adding very small additions of a very concentrated nitric acid solution and/or saturated KOH solution with negligible variation of the total volume and measured with a combined Crison 52 09 glass electrode (reference electrode Ag/AgCl). The electrode calibration was performed as described for potentiometry.

3. Results and Discussion

3.1. Models and Complexation Stability Constants. The complex formation in the metal $[\text{Co(II)}$, Cu(II) , and $\text{Ni(II)}]$ –BCIEE–OH (M –L–OH) systems has been followed by direct pH potentiometric titration. The comparative analysis between the experimental pH values recorded for the different metal–ligand titrations when compared with the pH titration of the ligand alone provides evidence that complexation between the BCIEE and the various metals begins in acidic conditions (between 2.5 and 4.6) for all ML systems (Figure 2).

The analysis of Figure 2 gives evidence of an accentuated sigmoidal pH versus a curves for the CuLOH system; this curve suggests the formation of only one strong major species, probably the CuL species, in the pH range between 4 and 10. On the other hand, pH versus a curves for the CoLOH and NiLOH systems gives evidence that BCIEE forms less stronger complexes with these two metal ions than with Cu(II) ions and suggests the formation of at least two species (Figure 2).

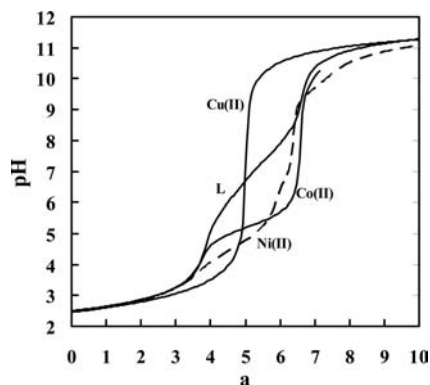


Figure 2. pH titrations of BCIEE with Cu(II), Co(II), and Ni(II), $[L_T]:[M_T] = 1$ and $[M_T] = 1.0 \cdot 10^{-3} \text{ mol} \cdot \text{L}^{-1}$; $\mu = 0.10 \text{ mol} \cdot \text{L}^{-1}$ (KCl) and $T = 25 \text{ }^\circ\text{C}$; $a =$ moles of base, potassium hydroxide, added per mole of ligand. For BCIEE alone, $[\text{BCIEE}] = 1.0 \cdot 10^{-3} \text{ mol} \cdot \text{L}^{-1}$.

Because BCIEE starts to complex Cu(II) at a very low pH, a variety of acidic monocomplexes, CuH_xL , could be formed. For the refinement operations of the CuLOH system, three models were assumed: model I [CuL and $\text{CuL}_x(\text{OH})_y$], model II [CuHL , CuL , and $\text{CuL}_x(\text{OH})_y$], and model III [CuH_2L , CuHL , CuL , and $\text{CuL}_x(\text{OH})_y$]. A tentative refinement of all the species included in the models over all the pH range was unsuccessful.

Since BCIEE forms strong complexes with Cu(II) ions (Figure 2), it was decided to refine the models [without including $\text{CuL}_x(\text{OH})_y$] over a narrow pH range (between 2.5 and 5.5). ESTA refined all three models (Table 3). The analysis of the results shows that the stability constant values obtained for the CuL species, by all three models, are equivalent. For model I, the analysis of the Z_M function (Figure 3) shows a very bad fit between the calculated and the experimental complexation curves for the whole refined pH range, which clearly indicates that this model was not the correct one. On the other hand, a mathematical compensation between the calculated and the experimental complexation curves for model II still occurred (Figure 3) and for lower pH values ($\text{pL} > 18.9$), the calculated Z_M function was below the experimental points; this fact indicates that another species should be formed in this pH range and can explain the observed mathematical compensation. Since a pL higher than 18.9 corresponds to pH values lower than 2.9, the missing species should correspond to a CuH_2L complex. In fact, a model constituted by CuH_2L , CuHL , and CuL species reproduced the experimental results well in the pH range considered (model III, Table 3 and Figure 3A). Additionally, Figure 3A indicates that, for higher pH values ($\text{pL} \leq 13.2$), Z_M values tend to 1, which indicates that for this pH or higher, CuL is totally formed.

To verify if model III was the correct model, a species distribution diagram (SDD) was drawn for $[L_T]:[\text{Cu}_T] = 1$, $[\text{Cu}^{2+}] = 1 \cdot 10^{-3} \text{ M}$ (Figure 4). The SDD shows that the formation of the CuH_2L species starts from pH 2 and reaches a

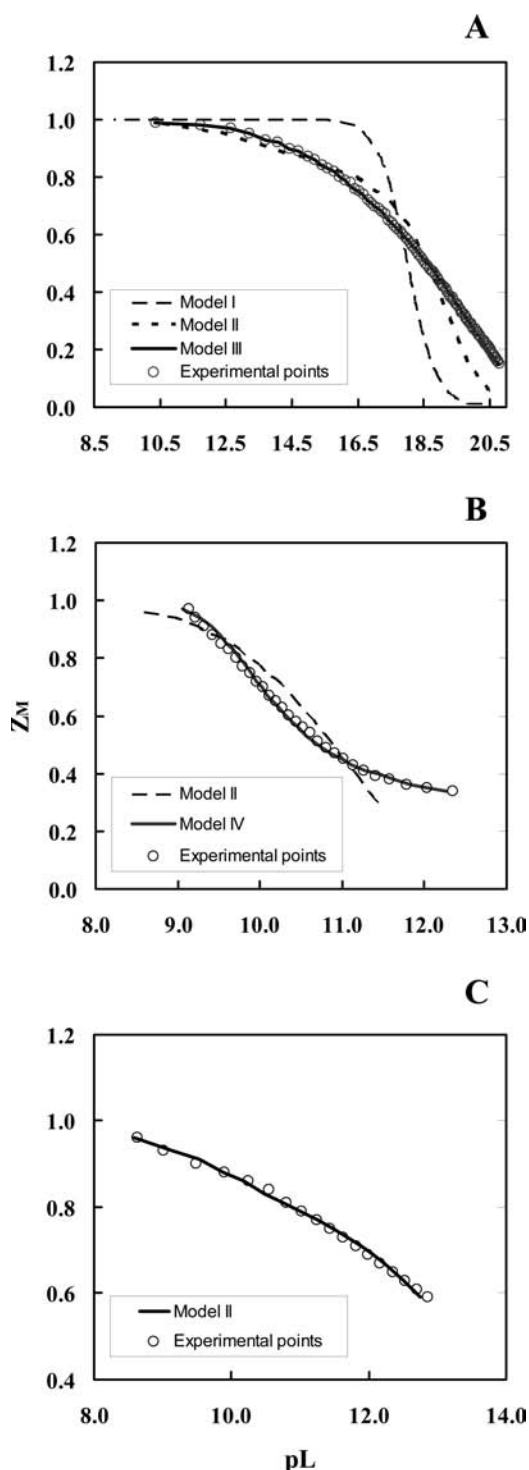


Figure 3. Z_M function for the (A) Cu(II)-BCIEE-OH, (B) Co(II)-BCIEE-OH, and (C) Ni(II)-BCIEE-OH systems. The computed Z_M functions were calculated from the refinement operations performed for models presented in Table 3. $[L_T]:[M_T] = 1$, $[M_T] = 1 \cdot 10^{-3} \text{ mol} \cdot \text{L}^{-1}$.

Table 3. Overall Stability Constants (as $\log \beta$ Values) for the M-BCIEE-OH Systems Determined by GEP in $0.1 \text{ mol} \cdot \text{L}^{-1}$ KCl at $25 \text{ }^\circ\text{C}$; M = Co(II), Cu(II), and Ni(II); $[L_T]:[M_T] = 1$; $[M_T] = 1 \cdot 10^{-3} \text{ mol} \cdot \text{L}^{-1}$

metal	Cu(II)			Co(II)		Ni(II)
	equilibrium	model I	model II	model III	model II	models III/IV
$\text{M}^{2+} + \text{L}^{2-} \leftrightarrow \text{ML}$	18.0 ± 0.1	17.91 ± 0.04	18.174 ± 0.003	10.83 ± 0.04	11.65 ± 0.02	12.72 ± 0.02
$\text{M}^{2+} + \text{L}^{2-} + \text{H}^+ \leftrightarrow \text{MLH}^+$	NI ^a	21.99 ± 0.03	22.200 ± 0.002	15.89 ± 0.09	R/NI	17.98 ± 0.02
$\text{M}^{2+} + \text{L}^{2-} + 2\text{H}^+ \leftrightarrow \text{MLH}_2^{2+}$	NI	NI	25.286 ± 0.004	NI	22.25 ± 0.02	NI/R
Hamilton R factor	0.055	0.014	0.00085	0.054	0.0094	0.0097
number of points	93	93	93	29	29	18
pH range	2.5 to 5.5	2.5 to 5.5	2.5 to 5.5	4.5 to 6.0	4.5 to 6.0	4.5 to 6.2

^a NI: not included, R: rejected.

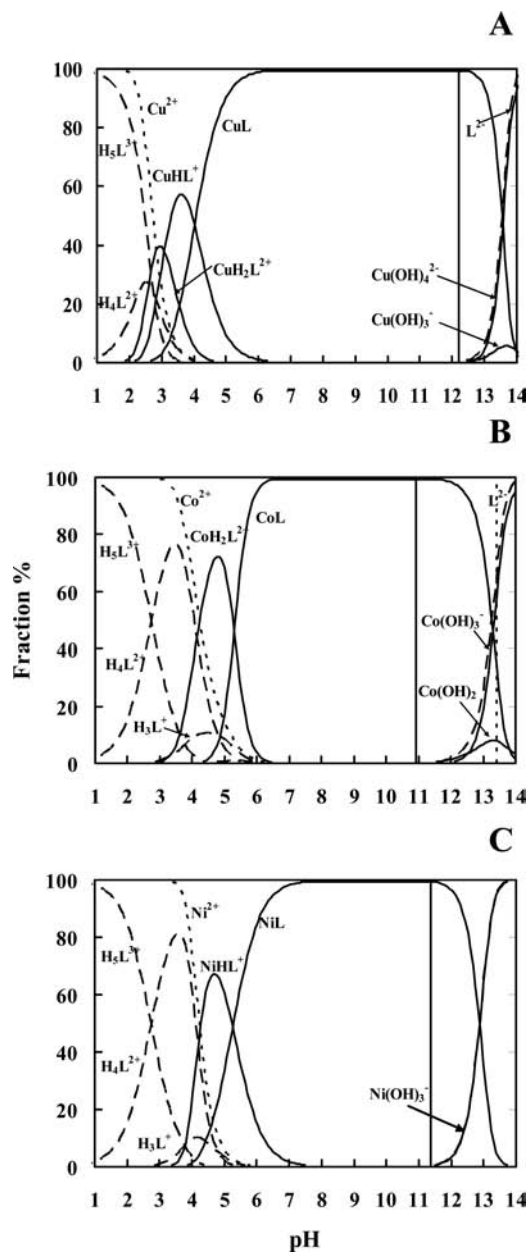


Figure 4. Species distribution diagrams computed for the various M-BCIEE-OH systems. (A) Cu-BCIEE-OH, (B) Co-BCIEE-OH, and (C) Ni-BCIEE-OH; $[L_T]:[M_T] = 1$, $[M_T] = 1.0 \cdot 10^{-3} \text{ mol} \cdot \text{L}^{-1}$. For all M-BCIEE-OH models, the overall stability constants, as $\log \beta$, are shown: (A) $\text{CuL} = 18.174$, $\text{CuLH} = 22.20$, and $\text{CuH}_2\text{L} = 25.286$, (B) $\text{CoL} = 11.65$ and $\text{CoLH}_2 = 22.25$, (C) $\text{NiL} = 12.72$ and $\text{NiLH} = 17.98$. The vertical lines indicate $\text{M}(\text{OH})_2$ precipitation (full line) and redissolution (dashed line).

maximum of about 40 % at pH 3. Consecutively, an exponential increase of CuHL and CuL species starts at pH 2.2 and 2.7, respectively. For pH values close to 6, about 100 % of the CuL species is formed. These results are in agreement with Figure 3, since for pL equal or lower than 10.3, which corresponds to a pH higher than 5.5, Z_M reaches a value of 1, which indicates that, for this pH or higher, the CuL species is totally formed. On the other hand, the SDD predicts the precipitation of $\text{Cu}(\text{OH})_2$ at pH 12, which is in agreement with our experimental observation. These results show that $\text{CuL}(\text{OH})_x$ species are not formed and the proposed final model should include the CuH_2L , CuHL, and CuL species. The final overall stability constants resulting from the refinement operations of all $[L_T]:[Cu_T]$ ratios are presented in Table 4.

Table 4. Overall Stability Constants (as $\log \beta$ Values) for BCIEE with Co(II), Cu(II), and Ni(II) Systems Determined by GEP in 0.1 $\text{mol} \cdot \text{L}^{-1}$ KCl at 25 °C

complexes	$\log \beta$
$\text{Cu}^{2+} + \text{L}^{2-} \leftrightarrow \text{CuL}$	18.0 ± 0.1
$\text{Cu}^{2+} + \text{L}^{2-} + \text{H}^+ \leftrightarrow \text{CuLH}^+$	22.10 ± 0.08
$\text{Cu}^{2+} + \text{L}^{2-} + 2\text{H}^+ \leftrightarrow \text{CuLH}_2^{2+}$	25.1 ± 0.1
number of points	452
number of titrations/number of independent solutions	5/3
$\text{Co}^{2+} + \text{L}^{2-} \leftrightarrow \text{CoL}$	11.91 ± 0.02
$\text{Co}^{2+} + \text{L}^{2-} + 2\text{H}^+ \leftrightarrow \text{CoLH}_2^{2+}$	22.45 ± 0.02
number of points	218
number of titrations/number of independent solutions	6/3
$\text{Ni}^{2+} + \text{L}^{2-} \leftrightarrow \text{NiL}$	12.70 ± 0.02
$\text{Ni}^{2+} + \text{L}^{2-} + \text{H}^+ \leftrightarrow \text{NiLH}^+$	18.10 ± 0.02
number of points	86
number of titrations/number of independent solutions	4/2

For the CoLOH and NiLOH systems, the pH versus a curve suggested the formation of at least two species (Figure 2). Thus, for the refinement operations of the MLOH systems two models were tested: model II [MHL, ML, and $\text{ML}_x(\text{OH})_y$] and model III [MH_2L , MHL, ML, and $\text{ML}_x(\text{OH})_y$]. Here again, similar to the CuLOH system, a tentative refinement of all of the species included in the models over all of the pH range was unsuccessful; then, models [without including $\text{ML}_x(\text{OH})_y$] were refined over a narrow pH range (Table 3). For the NiLOH system, NiH_2L was rejected in model III (Table 3); the refinement of model II resulted in stability constants with smaller standard deviations for both species and a perfect fit (Table 3 and Figure 3C). For the CoLOH system, CoHL was rejected in model III (Table 3). Then, the refinement operations for both simplified models (models II and IV) resulted in different and often acceptable models (Table 3). From this, it is obvious that additional information is required to suggest the most likely model. For this purpose, values of the complex formation function, Z_M , were calculated for each datum point to aid in the modeling procedures (see Figure 3B). The analysis of Figure 3B shows that the experimental Z_M functions (circles in Figure 3B) were reproduced fairly well with the model containing CoL and CoH_2L , for example, model IV in Table 3.

To test the proposed model, a SDD was generated for the experimental $[L_T]:[M_T]$ conditions used ($[L_T]:[M_T] = 1$, $[\text{M}^{2+}] = 1 \cdot 10^{-3} \text{ M}$) and assuming the final models proposed above: model II for the NiLOH system and model IV for the CoLOH system (Table 3). Figure 4 supports the models found at the $[L_T]:[M_T]$ ratio 1 for both MLOH systems. SDDs predict that complexation starts to occur at pH 3.0 to 3.5 for both MLOH systems, which is in agreement with the pH versus a curves (Figure 2). In addition, SDDs predict precipitation at pH 10.9 for the CoLOH and at pH 11.4 for the NiLOH systems, which is in agreement with our experimental observation. These results also corroborate that $\text{ML}(\text{OH})_x$ species are not formed.

After this exhaustive modeling exercise, the proposed final models should include the CoH_2L and CoL species, for the CoLOH system, and NiHL and NiL, for the NiLOH system. Overall stability constant values resulting from the refinement operations of all $[L_T]:[M_T]$ ratios are presented in Table 4.

3.2. UV-vis Spectroscopic Measurements. Analysis of the UV-vis spectra (Figure 5) obtained for all of the pH range studied clearly showed complexation among Co(II), Cu(II), and Ni(II) ions and BCIEE.

For the Cu(II)-BCIEE system, Figure 5A shows one single $d-d$ transition with a maximum wavelength of 812 nm at pH 1.5 (no complexation occurs; see Figure 4B), which is shifted to 667 nm at pH 2.5, where complexation of Cu(II) with BCIEE

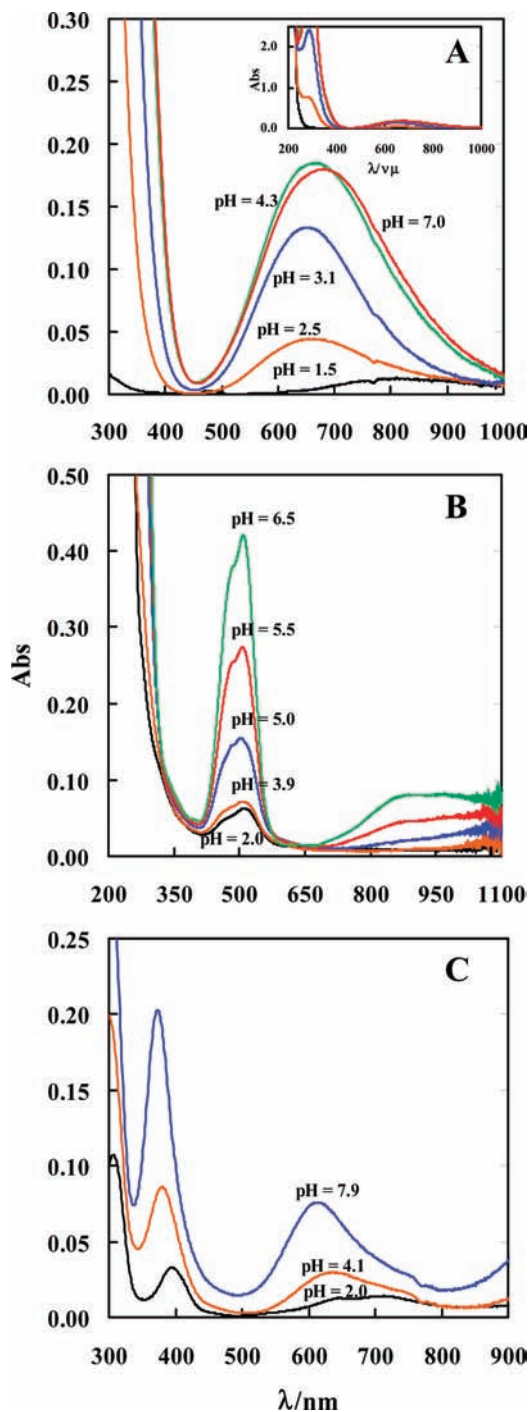


Figure 5. Spectrophotometric spectra obtained for (A) Cu(II)–BCIEE–OH [L_T]: $[M_T] = 1$, $[M_T] = 1.0 \cdot 10^{-3} \text{ mol} \cdot \text{L}^{-1}$, (B) Co(II)–BCIEE–OH, and (C) Ni(II)–BCIEE–OH systems; $[L_T]:[M_T] = 1.0$, $[M_T] = 1.0 \cdot 10^{-2} \text{ mol} \cdot \text{L}^{-1}$, in the case of the Ni(II)–BCIEE–OH and Co(II)–BCIEE–OH systems.

already occurs (Figure 4A). In addition to the blue shift of the $d-d$ transition, another band with a maximum at 280 nm (insert in Figure 5A) appeared. The position of this band and the magnitude of its molar absorptivity coefficient value ($\epsilon_{\text{max}} \cong 4000 \text{ mol}^{-1} \cdot \text{L} \cdot \text{cm}^{-1}$) suggests that it is a ligand-to-metal charge transference band [possibly carboxylate/copper(II)].^{21,22} Figure 5A shows that both bands at (280 and 650) nm increase with pH. Taking into account the proportions of the different species present at each pH value (Figure 4A), the ϵ_{max} values for each CuH_2L , CuHL , and CuL species were calculated and are presented in Table 5.

Table 5. UV–vis Spectral Parameters of the M(II)–BCIEE Complexes

metal/species	UV–vis	
	λ_{max} (nm)	ϵ ($\text{mol}^{-1} \cdot \text{cm}^{-1} \cdot \text{L}$)
Cu(II)–BCIEE:		
CuH_2L	667	170
CuHL	649	165
CuL	679	180
Co(II)–BCIEE:		
CoH_2L	502	8.3
CoL	509	42
Ni(II)–BCIEE:		
NiHL	380	11
	641	3.8
NiL	372	20.
	617	7.6

The BCIEE can act as a hexadentate ligand in aqueous solution (Figure 1). Two carboxylic groups ($\text{p}K_{\text{a}2} = 2.74$), two amine nitrogens ($\text{p}K_{\text{a}3} = 4.81$ and $\text{p}K_{\text{a}6} = 9.24$), and two imidazolyl nitrogens ($\text{p}K_{\text{a}4} = 6.04$ and $\text{p}K_{\text{a}5} = 7.21$) groups become available for complexation as the pH increases.¹⁸

If the logarithm of the H_2L protonation constant (Table 2) is subtracted from $\log \beta_{\text{CuH}_2\text{L}}$ (Table 4), the value obtained for CuH_2L is 8.62. This value is higher than the deprotonation constants of both carboxylic groups, as well as one of the amine and one imidazolyl nitrogen group in the “free” ligand.¹⁸ This fact raises two hypotheses for the structure of the CuH_2L complex. In the first one, the substitution of two water molecules from the equatorial plane of the copper aqueous complex, by one carboxylic and one amine groups forming a five-membered ring, can be hypothesized (left structure A, Figure 6). The value of the CuH_2L complex formation constant supports this interpretation since the $\log \beta_{\text{CuH}_2\text{L}}$ value (8.62) is much higher than the sum of the $\log \beta$ values of the individual coordination sites, CuCOO^- ($\log \beta_{\text{COO}^-} = 1.6$)²³ and CuN (amino) ($\log \beta_{\text{NH}_2} = 4.04$),²³ and is consistent with the stability constant value of a CuL glycine-type complex (8.19).²³ However, the λ_{max} of the $d-d$ transition determined for this complex (Table 5) does not suggest a glycine^{24–26} but a histamine-like coordination type.²⁷ The second hypothesis for the structure of the CuH_2L complex suggests the formation of a six-membered ring in the equatorial plane occupied by one amino and one imidazole nitrogen group (right structure A, Figure 6), that is, a histamine-like coordination type. The energy of the $d-d$ transition of the CuH_2L complex (Table 5) is similar to other complexes involving these donor groups,^{24,26} but the magnitude of the value of the CuH_2L complex formation constant (8.62) is lower than that obtained with a histamine-like coordination type (9.6).²³ These results suggest that CuH_2L exists in solution as an equilibrium mixture of both structures (Figure 6) and is consistent with the ambidentate nature of the histidine ligand, that is, the ability to coordinate histamine-like and glycine-like modes.²⁸

For CuHL complex, the magnitude of $\log \beta_{\text{CuHL}}$ (Table 4) indicates a strong increase in the stability, which corresponds to an increase in the donor groups around copper(II). In this complex, one amino group is still protonated.¹⁸ The values of ϵ_{max} and λ_{max} (Table 5), together with the increase of the charge transference band to Cu(II) due to the carboxylate group,^{21,22} suggest that the structure of the CuHL complex can be explained by assuming an equatorial plane occupied by one carboxylate, one amino, and one imidazole nitrogen group^{25,29} (Figure 6). Around pH 7 (at this pH, there is 99.9 % of CuL , Figure 4A), a red shift in the visible λ_{max} position of the copper(II) complex was recorded (Figure 5A). This red shift in the visible λ_{max} position of a copper(II) complex appears when a donor group

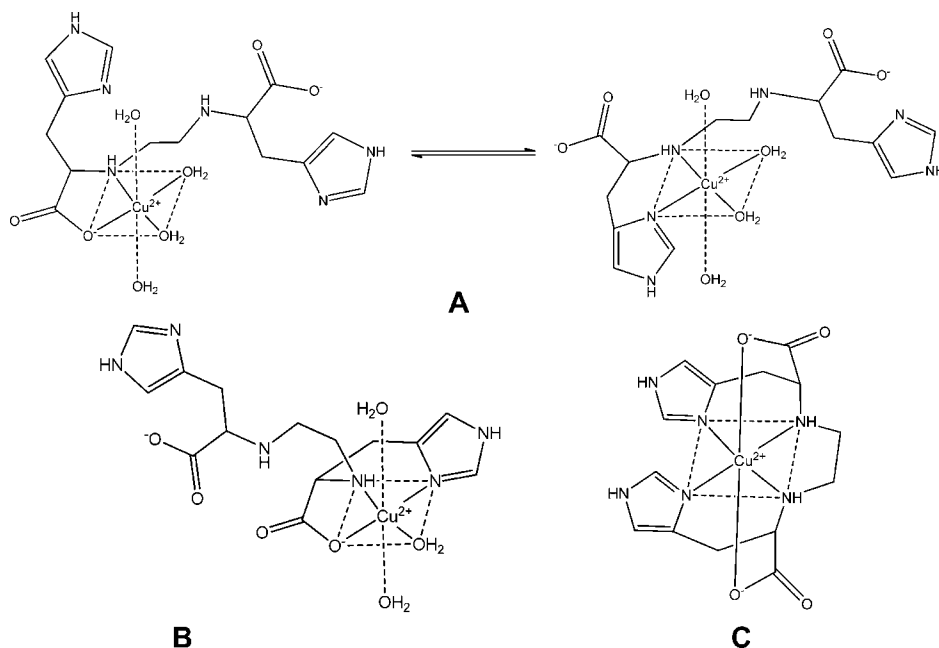


Figure 6. Possible structures of CuH_2L (A), CuHL (B), and CuL (C).

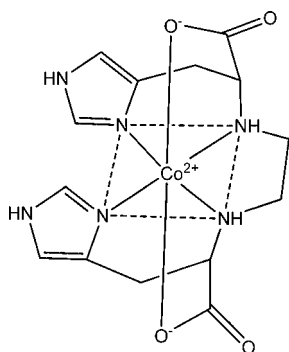


Figure 7. Possible structure of CoL .

is located in an axial position.^{30,31} In our context, this shift toward higher wavelengths, which is correlated with full CuL complex formation, points out a structural rearrangement of the equatorial coordinated acidic complexes (CuH_2L and CuHL) into a fully occupied distorted octahedron of copper(II). This fact is also compatible with the high stability constant value refined for CuL ($\log \beta = 18.0$; Table 4). Figure 6 shows the structure proposed for a CuL complex constituted by one five-membered chelate ring, composed of the two amino groups, plus two six-membered chelate rings, composed of the amino and imidazole groups, all in the equatorial copper(II) plane and two five-membered chelate rings, where the carboxylate groups of the ligand occupy apical positions.

The analysis of the Co(II) spectra (Figure 5B) obtained for all of the pH range studied clearly shows the formation of a complex between the cobalt(II) and the ligand around pH 5.0. The two bands that appear ($\lambda_{\text{max}} = 900 \text{ nm}$; $\lambda_{\text{max}} = 500 \text{ nm}$ with a shoulder around 475 nm) act in accordance as the expected energy range for the Co(II) $d-d$ transitions in high-spin octahedral cobalt complexes with four-fold nitrogen coordination in the equatorial plane and two oxygens in the axial plane (Figure 7). These data corroborate the high stability constant value refined for CoL (Table 4). Additionally, a comparison between the magnitude of the $\log \beta$ value (11.91) of the CoL species (Table 4) with the $\log \beta_{\text{CoL}_2}$ in Co -histidine ($\log \beta_{\text{CoL}_2} = 12.38$),²³ Co -histamine ($\log \beta_{\text{CoL}_2} = 8.75$),²³ and

Co -glycine ($\log \beta_{\text{CoL}_2} = 8.75$)²³ reinforces that BCIEE behaves as a hexadentate ligand via two COO^- , two NH_2 , and two N(Im) groups (Figure 7).

For the Ni(II) complexes, the analysis of the spectrum (Figure 5C) shows, at pH 2.0, the characteristic features of the nickel aquo complex, $\text{Ni(H}_2\text{O)}_6^{2+}$: two overlapped bands between (600 and 900) nm and a single one centered at 394 nm.³² At pH 4.1, the bands shift to lower wavelengths, and the overlapped ones result in a single transition centered at 630 nm with higher ϵ values. This spectrum corresponds mainly to the NiHL species. At pH 7.9, the bands shift to slightly lower wavelengths with a higher ϵ_{max} value. At this pH, this spectrum corresponds mainly to the NiL species. Since NiH_2L and NiL are the only species formed at pH 4.1 and 7.9, respectively, the ϵ_{max} values of these species were calculated and included in Table 5. The band positions as well as the ϵ_{max} values determined for the NiHL and NiL species (Table 5) correlate well with the octahedral coordination of Ni(II) ions.^{33,34} Further, the blue shift together with an increase in the ϵ_{max} values compared to that of the Ni(II) aquo complex indicates the involvement of nitrogen atoms in the coordination sphere of the NiHL and NiL species.^{34,35}

If the logarithm of the HL protonation constant is subtracted from $\log \beta_{\text{NiHL}}$, the obtained value for NiHL is 8.86. This stability constant value is similar to the stability constant value of NiL complex formed between nickel and histidine (8.66)²³ but much higher than the values determined with glycine (5.74) and histamine (6.82).²³ These results suggest that BCIEE behaves as a tridentate ligand via COO^- , NH_2 , and N(Im) groups, all in the equatorial plane. Figure 8 shows the proposed structure for the NiHL complex. On the other hand, the comparison between the $\log \beta$ value (12.70) of the NiL species (Table 4) with the $\log \beta_{\text{NiL}_2}$ in Ni -histidine ($\log \beta_{\text{NiL}_2} = 15.52$),²³ Ni -histamine ($\log \beta_{\text{NiL}_2} = 11.92$),²³ and Ni -glycine ($\log \beta_{\text{NiL}_2} = 10.58$)²³ systems suggests the involvement of the two NH_2 and the two N(Im) groups in the coordination sphere of the Ni^{2+} plane (Figure 8) and is in agreement with the UV-vis spectrum recorded (Figure 5C).

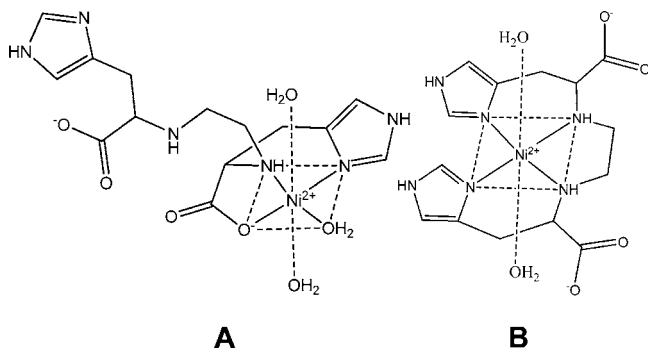


Figure 8. Possible structures of NiHL (A) and NiL (B).

4. Conclusions

We report here a potentiometric and UV–vis spectroscopic study of the coordination capability of a potentially hexadentate ligand, BCIEE, toward Cu(II), Co(II), and Ni(II) ions.

Potentiometric data revealed that BCIEE acts as a strong complexing agent for Cu(II), Co(II), and Ni(II) ions and allowed establishing the final models for all three M(II)–BCIEE systems. BCIEE starts to complex Cu(II), Co(II), and Ni(II) ions at very acidic pH conditions (pH 2, 3, and 3.5, respectively). In the case of the Cu(II)–BCIEE system, the refined overall stability constants were: $\log \beta_{\text{CuH}_2\text{L}} = 25.1 \pm 0.1$, $\log \beta_{\text{CuHL}} = 22.10 \pm 0.08$, and $\log \beta_{\text{CuL}} = 18.0 \pm 0.1$. For the Co(II)–BCIEE system, the refined overall stability constants values were: $\log \beta_{\text{CoH}_2\text{L}} = 22.45 \pm 0.02$ and $\log \beta_{\text{CoL}} = 11.91 \pm 0.02$. For the Ni(II)–BCIEE system, overall stability constant values were $\log \beta_{\text{NiH}_2\text{L}} = 18.10 \pm 0.02$ and $\log \beta_{\text{NiHL}} = 12.70 \pm 0.02$, respectively.

From the combined analysis of UV–vis and potentiometric data, coordination modes of the complexes were deduced. NiL involves the planar coordination of two imidazolyl and two amine nitrogen groups resulting in an octahedral geometry, where the apical positions are occupied by two water molecules. For both ML (CoL or CuL) complexes, all six donor groups of the BCIEE compound take place, resulting in an octahedral geometry. For MH_xL species, BCIEE behaves as a bidentate (in the case of CuH_2L species) or tridentate (in the case of MHL species) ligand. In these complexes, carboxyl group and/or imidazolyl and/or amino nitrogen atoms are coordinated to the metal ion with a square planar geometry.

Literature Cited

- Knepper, T. P. Synthetic chelating agents and compounds exhibiting complexing properties in the aquatic environment. 10. *Trends Anal. Chem.* **2003**, *22*, 708–724.
- Schmidt, C. K.; Fleig, M.; Sacher, F.; Brauch, H. E. Occurrence of aminopolycarboxylates in the aquatic environment of Germany. 1. *Environ. Pollut.* **2004**, *131*, 107–124.
- Nowack, B.; VanBriesen, J. M. Chelating agents in the environment. In *Biogeochemistry of chelating agents*; ACS Symposium Series 910; American Chemical Society: Washington, DC, 2005; Chapter 1.
- Pihko, P. M.; Rissa, T. K.; Aksela, R. Enantiospecific synthesis of isomers of AES, a new environmentally friendly chelating agent. 48. *Tetrahedron* **2004**, *60*, 10949–10954.
- Lutz, M.; Pursiainen, J.; Aksela, R. Facile syntheses of novel acyclic polycarboxylic acids. 4. *Z. Naturforsch., B: Chem. Sci.* **2005**, *60*, 408–412.
- Hyvonen, H.; Orama, M.; Arvelac, R.; Henriksson, K.; Saarinen, H.; Aksela, R.; Parene, A.; Jakara, J.; Renvall, I. Studies on three new environmentally friendly chelating ligands. 2. *Appita J.* **2006**, *59*, 142–149.
- Hyvonen, H.; Aksela, R. Complexation of [S,S,S]- and [R,S,R]-isomers of *N*-bis[2-(1,2-dicarboxyethoxy)ethyl] aspartic acid with Mg(II), Ca(II), Mn(II), Fe(III), Cu(II) and Zn(II) ions in aqueous solution. 16. *J. Coord. Chem.* **2008**, *61*, 2515–2527.
- Hyvonen, H.; Lehtinen, P.; Aksela, R. Complexation of *N*-bis[2-(1,2-dicarboxyethoxy)ethyl] aspartic acid with Cd(II), Hg(II) and Pb(II) ions in aqueous solution. 6. *J. Coord. Chem.* **2008**, *61*, 984–996.
- Metsarinne, S.; Ronkainen, E.; Tuhkanen, T.; Aksela, R.; Sillanpaa, M. Biodegradation of novel amino acid derivatives suitable for complexing agents in pulp bleaching applications. 1. *Sci. Total Environ.* **2007**, *377*, 45–51.
- Schowanek, D.; Feijtel, T. C. J.; Perkins, C. M.; Hartman, F. A.; Federle, T. W.; Larson, R. J. Biodegradation of [S,S], [R,R] and mixed stereoisomers of ethylene diamine disuccinic acid (EDDS), a transition metal chelator. 11. *Chemosphere* **1997**, *34*, 2375–2391.
- Barros, M. T.; Martins, J.; Pinto, R. M.; Santos, M. S.; Soares, H. Complexation Studies of *N,N'*-ethylenedi-L-cysteine with Some Metal Ions. 12. *J. Solution Chem.* **2009**, *38*, 1504–1519.
- Martins, J. G.; Pinto, R. M.; Gameiro, P.; Barros, M. T.; Soares, H. M. V. M. Equilibrium and solution structural studies of the interaction of *N,N'*-Bis(4-imidazolymethyl)ethylenediamine with Ca(II), Cd(II), Co(II), Cu(II), Mg(II), Mn(II), Ni(II), Pb(II) and Zn(II) metal ions. *J. Solution Chem.*, accepted for publication; reference: JOSL1119R1.
- O'Dowd, R. W.; Hopkins, D. W. Mineralization of carbon from D- and L-amino acids and D-glucose in two contrasting soils. 14. *Soil Biol. Biochem.* **1998**, *30*, 2009–2016.
- Williams, D. R. Speciation of chelating agents and principles for global environmental management. In *Biogeochemistry of chelating agents*; ACS Symposium Series 910; American Chemical Society: Washington, DC, 2005; Chapter 2.
- Pitter, P.; Sykora, V. Biodegradability of ethylenediamine-based complexing agents and related compounds. 4. *Chemosphere* **2001**, *44*, 823–826.
- Martell, A. E.; Hancock, R. D. *Metal Complexes in Aqueous Solutions*; Plenum Press: New York, 1996.
- Miyake, H.; Watanabe, M.; Takemura, M.; Hasegawa, T.; Kojima, Y.; Inoue, M. B.; Inoue, M.; Fernando, Q. Novel optically-active bis(amino acid) ligands and their complexation with gadolinium. 6. *J. Chem. Soc., Dalton Trans.* **2002**, 1119–1125.
- Takemura, M.; Yamato, K.; Doe, M.; Watanabe, M.; Miyake, H.; Kikunaga, T.; Yanagihara, N.; Kojima, Y. Europium(III)-*N,N'*-ethylenebis(L-amino acid) complexes as new chiral NMR lanthanide shift reagents for unprotected α -amino acids in neutral aqueous solution. 4. *Bull. Chem. Soc. Jpn.* **2001**, *74*, 707–715.
- May, P. M.; Murray, K.; Williams, D. R. The use of glass electrodes for the determination of formation constants - II. Simulation of titration data. 6. *Talanta* **1985**, *32*, 483–489.
- May, P. M.; Murray, K.; Williams, D. R. The use of glass electrodes for the determination of formation constants - III. Optimization of titration data: the ESTA library of computer programs. 11. *Talanta* **1988**, *35*, 825–830.
- Lever, A. *Inorganic electronic spectroscopy: studies in physical and theoretical chemistry*; Elsevier Science Publisher: Amsterdam, 1984; Vol. II.
- Prenci, E.; Berto, S. Interaction of copper(II) with imidazole pyridine nitrogen-containing ligands in aqueous medium: a spectroscopic study. *J. Inorg. Biochem.* **2002**, *88*, 37–43.
- Martell, A. E.; Smith, R. M. *NIST Standard Reference Database 46 Version 8.0, NIST Critically Selected Stability Constants of Metal Complexes Database*; U.S. Department of Commerce; National Institute of Standards and Technology: Gaithersburg, MD, 2004.
- Prenci, E.; Daniele, P. G.; Prenci, M.; Ostacoli, G. Spectrum-structure correlation for visible absorption spectra of copper(II) complexes in aqueous solution. 25. *Polyhedron* **1999**, *18*, 3233–3241.
- Prenci, E.; Daniele, P. G.; Toso, S. Visible spectrophotometric determination of metal ions: the influence of structure on molar absorptivity value of copper(II) complexes in aqueous solution. 2. *Anal. Chim. Acta* **2002**, *459*, 323–336.
- Kurzak, B.; Kamecka, A.; Bogusz, K.; Jezierska, J. Stabilities and coordination modes of histidine in copper(II) mixed-ligand complexes with ethylenediamine, diethylenetriamine or *N,N,N',N'',N'''*-pentamethyldiethylenetriamine in aqueous solution. 13. *Polyhedron* **2008**, *27*, 2952–2958.
- Goodman, B. A.; McPhail, D. B.; Powell, H. K. J. Electron-Spin Resonance Study of Copper(II)-Amino-Acid Complexes - Evidence for Cis-Isomers and Trans-Isomers and the Structures of Copper(II)-Histidinate Complexes in Aqueous-Solution. 3. *J. Chem. Soc., Dalton Trans.* **1981**, 822–827.
- Altun, Y.; Koseoglu, F. Stability of copper(II), nickel(II) and zinc(II) binary and ternary complexes of histidine, histamine and glycine in aqueous solution. 2. *J. Solution Chem.* **2005**, *34*, 213–231.
- Prenci, E.; Daniele, P. G.; Berto, S.; Toso, S. Spectrum-structure correlation for visible absorption spectra of copper(II) complexes showing axial co-ordination in aqueous solution. 15. *Polyhedron* **2006**, *25*, 2815–2823.

- (30) Jorgensen, C. K. Comparative crystal field studies II. Nickel(II) and copper(II) complexes with polydentate ligands and the behaviour of the residual places of co-ordination. 6. *Acta Chem. Scand.* **1956**, *10*, 887–910.
- (31) Bjerrum, J.; Ballhausen, K.; Jorgensen, C. Studies on absorption spectra. I. Results of calculations on the spectra and configuration of copper(II) ions. 7. *Acta Chem. Scand.* **1954**, *8*, 1275–1289.
- (32) Gushikem, Y. Electronic spectra of some Ni²⁺ octahedral complexes: A practical introduction to the crystal field theory in the undergraduate course. 1. *Quim. Nova* **2005**, *28*, 153–156.
- (33) Gergely, A.; Sovago, I. Thermodynamic and structural study of the parent and some mixed ligand complexes of histamine and 1,3-diaminopropane with copper(II) and nickel(II) ions. 1. *Inorg. Chim. Acta* **1976**, *20*, 19–25.
- (34) Conato, C.; Ferrari, S.; Kozlowski, H.; Pulidori, F.; Remelli, M. Ni(II) complexes of dipeptides: a thermodynamic and spectroscopic study. 7–8. *Polyhedron* **2001**, *20*, 615–621.
- (35) Jezowska-Bojczuk, M.; Kaczmarek, P.; Bal, W.; Kasprzak, K. S. Coordination mode and oxidation susceptibility of nickel(II) complexes with 2'-deoxyguanosine 5'-monophosphate and L-histidine. 11. *J. Inorg. Biochem.* **2004**, *98*, 1770–1777.
- (36) Martell, A. E.; Smith, R. M. *NIST Standard Reference Database 46 Version 3.0, NIST Critically Selected Stability Constants of Metal Complexes Database*; U.S. Department of Commerce; National Institute of Standards and Technology: Gaithersburg, MD, 1997.

Received for review February 9, 2010. Accepted June 4, 2010. Financial support by FCT (Projects POCI/QUI/57891/2004 and PPCDT/QUI/57891/2004) with FEDER funds are gratefully acknowledged. One of us (J.G.M.) also gratefully acknowledges a grant scholarship financed under the same projects. We also thank Professor Carlos Gomes from University of Porto (Portugal) for the COPOTISY program.

JE1001494